# Conformational Analysis of LYS(11−36), a Peptide Derived from the β-Sheet Region of T4 Lysozyme, in TFE and SDS[†]

Lidia V. Najbar,[‡] David J. Craik,[‡,§] John D. Wade,[||] Daniella Salvatore,[||] and Michael J. McLeish*[,‡]

*Victorian College of Pharmacy, Monash University, 381 Royal Pde, Parkville 3052, Australia, and Howard Florey Institute, University of Melbourne, Parkville 3052, Australia*

ABSTRACT: The solution conformation of a peptide LYS(11−36), which corresponds to the β-sheet region in T4 lysozyme, has been examined in aqueous solution, TFE, and SDS micelles by CD and ^{1}H NMR spectroscopy. Secondary structure predictions suggest some β-sheet and turn character in aqueous solution but predict a helical conformation in a more hydrophobic environment. The predictions were supported by the CD and NMR studies which showed the peptide to be relatively unstructured in aqueous solution, although there was some evidence of a β-turn conformer which was maintained in 200 mM SDS and, to a lesser extent, in 50% TFE. The peptide was significantly helical in the presence of either 50% TFE or 200 mM SDS. TFE and SDS titrations showed that the peptide could form helical, sheet, or extended structure depending on the TFE or SDS concentration. The studies indicate that peptide environment is the determining factor in secondary structure adopted by LYS(11−36).

It is now well over 20 years since it was shown that the amino acid sequence of a protein determined its native structure (Anfinsen, 1973). In that time, much effort has been expended in (i) predicting the secondary structure of proteins and (ii) identifying those regions of secondary structure which may provide initiation sites for the folding of the rest of proteins. Current *a priori* predictions are about 70% accurate at predicting secondary structure from amino acid sequence (Waterhous & Johnson, 1994). However, it may prove impossible to attain 100% accuracy as there is an inherent difficulty in including nonlocal as well as local interactions in the calculations (Rao *et al.*, 1993; Waterhous & Johnson, 1994). Almost certainly, it will prove to be at least as difficult to predict the order in which those elements of secondary structure will form, an important consideration as hierarchical folding models (Kim & Baldwin, 1982, 1990) require the initial formation of secondary structure which can act as nucleation sites for further collapse, leading to native tertiary structure. Both stopped-flow CD and pulsed hydrogen-deuterium (HD)[1] exchange NMR experiments have proved useful to demonstrate that a high degree of secondary structure may form within milliseconds of protein folding being initiated. The latter technique, in particular, is presently limited to proteins of relatively low molecular weight and, consequently, is not generally applicable. In addition, both techniques have a dead time and events earlier than 1 ms simply cannot be observed.

An alternative means of identifying initiation sites for protein folding is to use short peptides which encompass known regions of secondary structure. Since CD and NMR spectroscopy were used to detect a highly populated β-turn in a 9-residue peptide in water (Dyson *et al.*, 1985), a substantial number of short peptides have been shown to adopt secondary conformation (e.g., α-helices and β-turns) in aqueous solution (Oas & Kim, 1988; Dyson & Wright, 1991; Dyson *et al.*, 1992a,b; Waltho *et al.*, 1993; Kemmink & Creighton, 1995). Subsequently, it was suggested that peptides based on native sequence, and showing a propensity for native-like conformation in the absence of stabilizing tertiary interactions, could be used to identify initiation sites for the folding of the parent protein (Wright *et al.*, 1988; Dyson & Wright, 1993). This approach has been used in attempts to identify initiation sites for the folding of proteins such as myoglobin (Waltho *et al.*, 1993), hen lysozyme (Yang *et al.*, 1994), β-lactoglobin (Hamada *et al.*, 1995), and BPTI (Kemmink & Creighton, 1995).

In testing the propensity of peptides for secondary structure formation, the addition of cosolvents to aqueous solutions has become very common. In particular, 2,2,2-trifluoroethanol (TFE) has been used routinely to promote α-helical conformation in peptides that have an intrinsic helical propensity, but are unstructured in aqueous solution (e.g., Dyson *et al.*, 1992a,b; Sönnichsen *et al.*, 1992). It has been generally accepted that TFE does not induce helical structure, rather it stabilizes helices in regions with an existing α-helical propensity (Segawa *et al.*, 1991; Sönnichsen *et al.*, 1992). TFE is not limited to promoting helix formation as it has

---

* Author to whom correspondence should be addressed.
[‡] Victorian College of Pharmacy.
[||] Howard Florey Institute.
[§] Present address: Center for Drug Design and Development, University of Queensland, Brisbane 4072, Australia.
[⊗] Abstract published in *Advance ACS Abstracts,* September 1, 1997.

[1] Abbreviations: CD, circular dichroism; NMR, nuclear magnetic resonance; TFE, 2,2,2,-trifluoroethanol; SDS, sodium dodecyl sulfate; NOE, nuclear Overhauser effect; NOESY, two-dimensional nuclear Overhauser spectroscopy; TOCSY, total correlation spectroscopy; COSY, two-dimensional correlated spectroscopy; DQF-COSY, double-quantum-filtered COSY; DIPSI, decoupling in the presence of scalar interactions; FID, free induction decay; 2D, two-dimensional; TSP, 3-(trimethylsilyl)propionic acid-2,2,3,3-$d_4$ sodium salt; HD, hydrogen-deuterium; BPTI, bovine pancreatic trypsin inhibitor; cmc, critical micellar concentration.

also been shown to stabilize β-turns (Blanco *et al.*, 1994a,b; Blanco & Serrano, 1995) and even β-strands (Lu *et al.*, 1984; Martenson *et al.*, 1985; Mutter & Altman, 1985; Narayanan *et al.*, 1986). Similarly, above its critical micellar concentration (cmc), sodium dodecyl sulfate (SDS) has also been used to stabilize peptides in helical conformations (Gierasch, 1989; Mammi & Peggion, 1990; Rizo *et al.*, 1993), while below its cmc, SDS has been shown in some cases to stabilize β-strands (Wu *et al.*, 1981, 1982; Zhong & Johnson, 1992; Waterhous & Johnson, 1994).

Previously, we have reported CD and NMR studies on the solution conformations of peptides derived from helical regions of T4 lysozyme, a small highly structured protein consisting of eight helices and one region of antiparallel β-sheet (Remington & Matthews, 1978; Weaver & Matthews, 1987). These peptides, which corresponded to helix A (McLeish *et al.*, 1993), helix B (Najbar *et al.*, 1995), and helix C (McLeish *et al.*, 1994), were found to exhibit only marginal, if any, structure in water. However, in the presence of SDS micelles or TFE, the peptides adopted relatively stable helical conformations. On the basis of these studies we proposed that helices A and C may provide initiation sites for the refolding of T4 lysozyme (McLeish *et al.*, 1993, 1994). These results provided support for earlier HD exchange studies in which helices A and C were found to be well protected from exchange, also suggesting that these helices form early in the folding of T4 lysozyme (Lu & Dahlquist, 1992). The HD exchange experiments also indicated that the β-sheet region folded rapidly (Lu & Dahlquist, 1992) and, in addition, a recent theoretical study predicted that this region would form part of an early folding intermediate (Xie & Freire, 1994). Given these results, it seemed to us that the conformational preferences of a peptide corresponding to the sheet region would warrant investigation.

Accordingly, we have used CD and 2D NMR spectroscopy to determine the solution structure of such a peptide, LYS-(11−36), in water, in 50% TFE and in SDS micelles. In addition, it seems that examining alterations in conformation brought about by controlled changes in its environment will provide us with physical evidence of the propensity of a peptide to adopt a given conformation and, conceivably, a better guide to potential initiation sites. Consequently, we have used CD spectropolarimetry to study the effect of TFE and SDS concentration on the conformation of LYS(11−36) and contrasted these effects with those on LYS(59−81), a peptide derived from helix C, the long helix bridging the two domains of T4 lysozyme.

## EXPERIMENTAL SECTION

*Peptide Synthesis.* LYS(59−81) was available from a previous study (McLeish *et al.*, 1994). LYS(11−36), EG-LRLKIYKDTEGYYTIGIGHLLTKS, was assembled by Fmoc-solid phase synthesis on a MilliGen 9050 instrument using previously described methodology (Wade *et al.*, 1995). It was cleaved from the solid support and simultaneously deprotected by treatment for 3.5 h with 95% trifluoroacetic acid/2.5% phenol/2.5% ethanethiol. The crude product was purified by preparative reversed phase high performance liquid chromatography (RP-HPLC) on a Vydac C18 support using 0.1% aqueous trifluoroacetic acid and acetonitrile. The resulting product appeared as a single peak on both analytical RP-HPLC and capillary zone electrophoresis (pH 2.5).

Amino acid analysis of a 24 h acid hydrolyzate gave (theoretical values in parenthesis) Asp (1) 1.04, Thr (3) 3.03, Ser (1) 1.00, Glu (2) 2.09, Gly (4) 3.92, Ile (3) 2.93, Leu (4) 4.12, Tyr (3) 2.81, His (1) 1.02, Lys (3) 3.01, and Arg (1) 0.95. Ion-spray mass spectrometry gave a $m/z$ of 2969.5 (theoretical value = 2967.6).

*CD Spectropolarimetry.* CD spectra were recorded on a Jasco J-710 spectropolarimeter. The instrument was calibrated using *d*-10-camphorsulfonic acid. Cells having a path length of 0.1 or 0.02 cm were employed and were maintained at the required temperature using a Neslab RTE-110 circulating water bath. Peptide concentrations were between 25 and 250 $\mu$M and were determined by amino acid analysis. Spectra were an average of five scans recorded at a scan speed of 20 nm/min, with a band width of 1.0 nm, a 0.2 nm step size, and a 2 s time constant. Following baseline correction, the observed ellipticity was converted to mean residue ellipticity, $[\theta]$ (deg cm$^2$ dmol$^{-1}$) using the relationship $[\theta] = \theta/(lcN)$, where $\theta$ is the observed ellipticity, $l$ is the path length in millimeters, $c$ is the molar concentration, and $N$ is the number of residues in the peptide. If necessary, the spectra were smoothed using the Jasco software.

*Secondary Structure Predictions.* The conformational preferences of LYS(11−36) were simulated using the program ALB (Ptitsyn & Finkelstein, 1983). This program can be used to predict elements of secondary structure based on the physicochemical properties of peptides when they are placed in aqueous, partially hydrophobic, and fully hydrophobic environments.

*$^1$H NMR Spectroscopy.* Peptide solutions were prepared to a concentration of 1−2 mM in a volume of 0.65 mL. The solvents employed included 90% H$_2$O/10% D$_2$O (pH 3.17), 45% 5 mM KPO$_4$ (pH 3.35)/50% TFE/5% D$_2$O, and deuterated 200 mM SDS micelles in 90% H$_2$O/10% D$_2$O (pH 4.5). For the slow exchange experiments, samples were prepared in 50% TFE/50% D$_2$O or 200 mM SDS-$d_{25}$/100% D$_2$O.

The $^1$H NMR spectra were recorded on Bruker AMX 500 and 600 MHz spectrometers at 288 K (298 K for SDS samples), with time proportional phase incrementation (TPPI) for quadrature detection in the F1 dimension (Wüthrich, 1986). DQF-COSY (Rance *et al.,* 1983) and TOCSY (Braünschweiler & Ernst, 1983; Bax & Davis, 1985) experiments, the latter using a DIPSI spin-locking sequence (Cavanagh & Rance, 1992), were used for spin system assignment. Phase-sensitive NOESY (Kumar *et al.,* 1980) was used to obtain complete sequence specific assignments and for providing conformational information. The mixing times ranged from 70 to 100 ms for the TOCSY experiments and 200 to 250 ms for NOESY experiments.

For DQF-COSY experiments, the water resonance was suppressed by gated irradiation during the relaxation delay (1.8−2 s), with the transmitter offset placed to coincide with the water resonance. Solvent suppression for NOESY and TOCSY experiments was achieved using a 1-1 binomial pulse sequence in place of the 90° pulse (Plateau & Gueron, 1982), combined with mild presaturation (1.5 s). Spectra were acquired with 4K complex data points in the F2 dimension and 256−600 increments in the F1 dimension, and were of 32 scans each (between 64−72 scans for NOESY).

All spectra were processed using UXNMR (Bruker) and FELIX (Hare Research Inc.) software. For 2D experiments, the $t_1$ dimension was zero-filled to 2048 real data points and

Table 1:  Secondary Structure Prediction for LYS(11−36)[a,b]

| | E1 | G2 | L3 | R4 | L5 | K6 | I7 | Y8 | K9 | D10 | T11 | E12 | G13 | Y14 | Y15 | T16 | I17 | G18 | I19 | G20 | H21 | L22 | L23 | T24 | K25 | S26 |
|---|---|---|---|---|---|---|---|---|---|---|---|---|---|---|---|---|---|---|---|---|---|---|---|---|---|---|
| aqueous | | | | | | B | B | B | B | B | B | T | T | T | B | B | B | & | & | & | & | & | & | | | |
| partially hydrophobic | | | B | B | B | B | B | B | T | T | T | T | B | B | B | B | T | T | & | & | & | & | & | | | |
| fully hydrophobic | | | & | & | & | & | & | & | T | T | T | T | T | H | H | H | H | H | H | H | H | H | H | | | |

[a] Calculated using the ALB algorithm (Ptitsyn & Finkelstein, 1983), using a temperature of 288 K and pH 4.8. H, helix predicted; &, helix possible; B, sheet predicted; T, turn predicted.
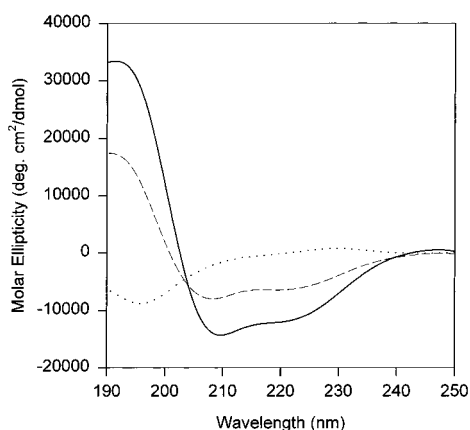


FIGURE 1:  Far-UV CD spectra of LYS(11−36) at 288 K in (···) phosphate buffer pH 4.8, (---) 200 mM SDS micelles, and (—) 10 mM phosphate buffer, pH 4.8/50% TFE. The molar ellipticity is in deg cm$^2$ dmol$^{-1}$.

$\pi/2$ phase shifted sine squared window functions were applied. In the cases of severe spectral overlap, $\pi/4$ or $\pi/8$ phase shifted sine squared bell window functions in F2 dimension were applied. Polynomial baseline correction was applied in selected regions of the spectra. Chemical shifts were referenced to 3-(trimethylsilyl)propionic acid-2,2,3,3-$d_4$ sodium salt (TSP-$d_4$) at 0.0 ppm.

## RESULTS

*Structure Prediction.* Table 1 shows the secondary structure predicted by the program ALB (Ptitsyn & Finkelstein, 1983) for LYS(11−36) in an aqueous, partially hydrophobic and fully hydrophobic environment. ALB predictions are based on physicochemical properties and can take into account environmental conditions. Simulations were carried out using charged termini, at 288 K, and at a pH of 4.8, i.e., under conditions designed to mimic CD experiments.

In water, ALB suggests that the peptide would have two regions of sheet, between residues 6 and 11 and residues 15−17, connected with a turn between residues 12 and 14. There is a possibility of a region of helix between residues 18−23, although a helix was not specifically predicted. As the hydrophobicity of the environment was increased, the predicted region of sheet and turn increased to include residues 3−18, while residues 19−23 maintained a possibility of helix formation. However, at maximum hydrophobicity, helix was predicted for residues 14−23, the possibility of helix was suggested for residues 3−8, and only residues 9−13 retained any tendency toward sheet or turn formation.

*CD Spectropolarimetry.* Figure 1 shows CD spectra of LYS(11−36) at 288 K in aqueous solution, in 50% TFE, and in 200 mM SDS. The water spectrum shows a minimum at 197 nm and is consistent with the peptide adopting a predominantly random coil conformation (Woody, 1985). Upon addition of 50% TFE, the spectrum becomes indicative of the peptide adopting a helical conformation, as the

minimum has shifted to 209 nm ($\pi\pi^*$ transition) and considerable negative ellipticity has developed at 222 nm ($n\pi^*$ transition). The shift toward a helical conformation is also evident in 200 mM SDS, with minima also being observed at 208 and around 222 nm, but the extent of helix formation is clearly lower. Under these solvent conditions, the CD spectra were essentially independent of peptide concentration, suggesting aggregation was not occurring.

If it is assumed that the absorption at 222 nm is almost exclusively due to $\alpha$-helix (Woody, 1985), it is possible to calculate the $\alpha$-helicity using the equation of Chen *et al.* (1974),

$$[\theta]_\lambda = (f_\mathrm{H} - ik/N)[\theta]_{\mathrm{H}\lambda\infty}$$

where $[\theta]_\lambda$ is the observed mean residue ellipticity at wavelength $\lambda$, $f_\mathrm{H}$ is the fraction of helix, $i$ is the number of helical segments (1 in this case), $k$ is a wavelength-dependent constant, $N$ is the number of residues, and $[\theta]_{\mathrm{H}\lambda\infty}$ is the maximum mean residue ellipticity for a helix infinite length. On this basis, $[\theta]_{222}$ for LYS(11−36) in a 100% helical conformation was calculated to be −35 550 deg cm$^2$ dmol$^{-1}$. From the observed $[\theta]_{222}$ data, at 288 K, the population averages of helical conformations in water, 50% TFE, and 200 mM SDS were approximately 0, 33, and 18%, respectively.

Figure 2 shows the CD spectra of (A) LYS(11−36) and (B) LYS(59−81) in the presence of increasing concentrations of TFE. Both peptides show increased helicity at higher TFE concentrations. However, there are some significant differences between the peptides. LYS(59−81) reaches maximum helicity at 30−40% TFE. This is consistent with the suggestion by Jasanoff and Fersht (1994) that helicity is generally at a maximum by 20−30% TFE (v/v) and complete by 50% TFE. In contrast, the helicity of LYS(11−36) increases continually over the range 30−80% TFE. Further, at 20% TFE, the spectrum of LYS(11−36) shows a minimum at 216 nm, typical of $\beta$-strand formation (Woody, 1985; Waterhous & Johnson, 1994). This is not observed for LYS-(59−81), where the presence of an isodichroic point indicates this peptide undergoes a simple random coil/helix transition (Waltho *et al.*, 1993; McLeish *et al.*, 1994).

Figure 3 shows (A) LYS(11−36) and (B) LYS(59−81) in the presence of increasing concentrations of SDS micelles. At concentrations around and above 6 mM SDS, the critical micellar concentration (Tessari *et al.*, 1993), both peptides fold into $\alpha$-helical conformations. Again, LYS(59−81) showed considerably greater helicity than LYS(11−36). However, below the cmc the two peptides exhibited quite different spectra. At 3 mM SDS, LYS(11−36) showed a minimum around 216−218 nm and a maximum below 195 nm. This is consistent with the peptide adopting a $\beta$-strand conformation, and has been observed previously for a number of peptides in nonmicellar SDS (Wu *et al.*, 1981; Zhong & Johnson, 1992; Waterhous & Johnson, 1994). As the SDS concentration is further decreased, the maximum shifts
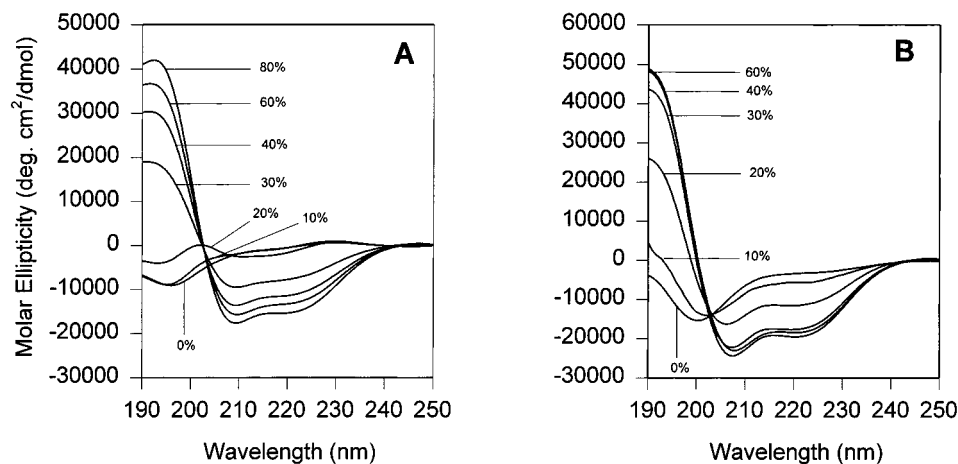
FIGURE 2: TFE titration of (A) LYS(11−36) and (B) LYS(59-81) at 288 K. The peptide concentrations were 28.5 and 32 $\mu$M, respectively.
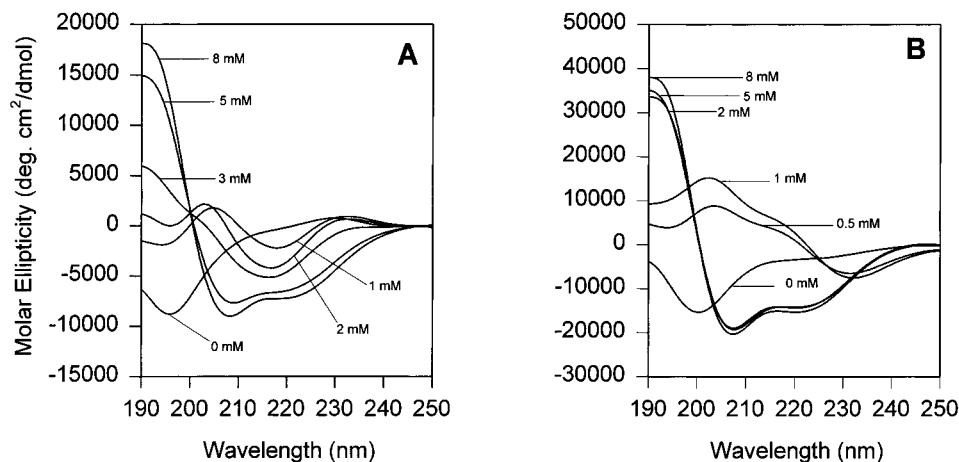


FIGURE 3: SDS titration of (A) LYS(11−36) and (B) LYS(59-81) at 288 K. The peptide concentrations were 28.5 and 32 $\mu$M, respectively.

toward 205−208 nm and the minimum also shifts toward longer wavelengths. This could indicate a flattening or twisting of the $\beta$-sheet (Manning *et al.*, 1988) and/or an increasing population of type II $\beta$-turn conformers (Bandekar *et al.*, 1982). At this point, if higher concentrations of SDS are added, the helical spectrum is restored (data not shown). LYS(59−81), on the other hand, maintains its helical conformation even at 2 mM SDS. Further reduction in the SDS concentration results in spectra showing a maximum at 205 nm and a minimum around 230 nm, indicative of a large population of $\beta$-structures (Bandekar *et al.*, 1982). However, under these conditions, the peptide/SDS solutions rapidly show signs of turbidity and, within a few hours, precipitates which cannot be reversed with the addition of higher concentrations of SDS are observed.

*¹H NMR Spectroscopy.* Spectra of LYS(11−36) were assigned using standard sequential assignment methods (Wüthrich, 1986). The assignment procedure was complicated by the degeneracy of the peptide sequence which contains multiple leucine, isoleucine, tyrosine, glycine, and lysine residues. However, these ambiguities were overcome by the identification of medium-range NOEs such as $d_{\alpha N}(i,i + 2)$, $d_{\alpha N}(i,i + 3)$, and $d_{\alpha\beta}(i,i + 3)$, and sequential NOEs such as $d_{NN}(i,i + 1)$ and $d_{\beta N}(i,i + 1)$ NOEs. Chemical shifts for LYS(11−36) in $H_2O$, 50% TFE and 200 mM SDS are provided in a table as Supporting Information.

*$H_2O$, 288 K.* The C$\alpha$H-NH region of the NOESY spectrum of LYS(11−36) in $H_2O$ is shown in Figure 4. This spectrum illustrates the sequential assignment and identifies some of the shorter range NOEs. As depicted in Figure 4,
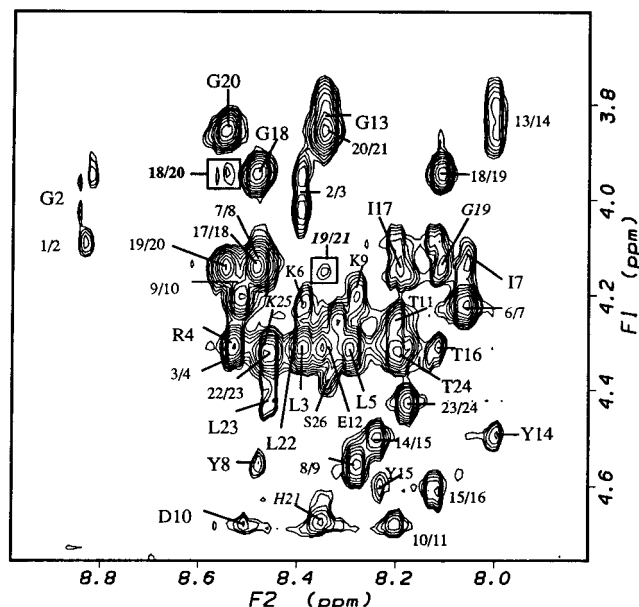


FIGURE 4: The C$\alpha$H-NH region of a NOESY spectrum for LYS-(11−36) in $H_2O$ (pH 3.17) at 283 K, showing the sequential assignment. The two weak $d_{\alpha N}(i,i + 2)$ NOEs referred to in the text are shown in boxes.

two weak $d_{\alpha N}(i,i + 2)$ NOEs were observed between residues G18/G20 and I19/H21, suggesting that a turn may be present at these residues. A turn is present in the corresponding region of the crystal structure in T4 lysozyme, which involves residues Gly28-Ile29-Gly30-His31. A complete representation of observed NOEs for LYS(11−36) in $H_2O$ is sum-
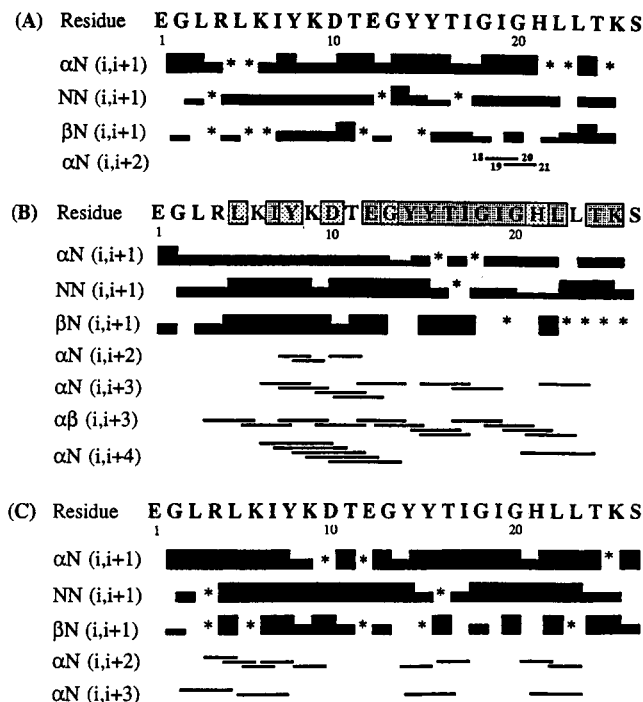
FIGURE 5: Summary of NOE and amide proton exchange data for LYS(11−36) in three solvents: (A) H₂O (pH 3.17), 283 K, (B) 50% TFE (pH 3.35), 288 K, and (C) 200 mM SDS micelles (pH 4.5), 298 K, 600 MHz. NOE intensity is indicated by the height of the bars. Overlapped residues are marked by asterisks. Dark and light shaded boxes indicate residues for which slow (present ≥ 4 h) and moderately slow (present 0.5−2 h) NH exchange was observed, respectively.

marized in Figure 5A. Overall, the observation of relatively strong $d_{αN}(i,i + 1)$ NOEs, weaker $d_{NN}(i,i + 1)$ NOEs, and lack of medium-range NOEs suggests that, in accord with the CD data, the peptide is predominantly disordered in aqueous medium.

The conformation of peptides can often be deduced from secondary chemical shifts (i.e., chemical shift differences from random coil values). Generally, upfield shifts are experienced by CαH protons within an α-helical conformation and downfield shifts are experienced by CαH protons in an extended or β-strand conformation (Wishart *et al.*, 1991, 1992). The chemical shift index (CSI) method of Wishart et al. (1992) provides a convenient way of using this chemical shift information to indicate secondary structure. In this method, values of four consecutive "−1s" are indicative of helix, 0 is indicative of random coil or helix disruption, and four consecutive "+1s" are indicative of β-sheet. A sudden positive to negative change in the CSI is indicative of a β-turn (Wishart *et al.*, 1992). Figure 6 shows the CSI for LYS(11−36) in aqueous solution, 50% TFE, and SDS micelles. The index is in agreement with LYS(11−36) being generally in an extended conformation in water. In addition, a sudden positive to negative change in the CSI involving residues 5−7 and 19−21 is indicative of β-turns, with the existence of the latter turn supported by the I19/H21 NOE connectivity observed in the NOESY spectrum.

*50% TFE, 288 K.* The NOEs for LYS(11−36), in 50% TFE, are summarized in Figure 5B and portions of NOESY spectra are shown in Figure 7. Many medium-range NOEs, including several $d_{αβ}(i,i + 3)$ NOEs, as well as a significant number of slowly exchanging NH protons, indicate the presence of a large population of helical conformers for this
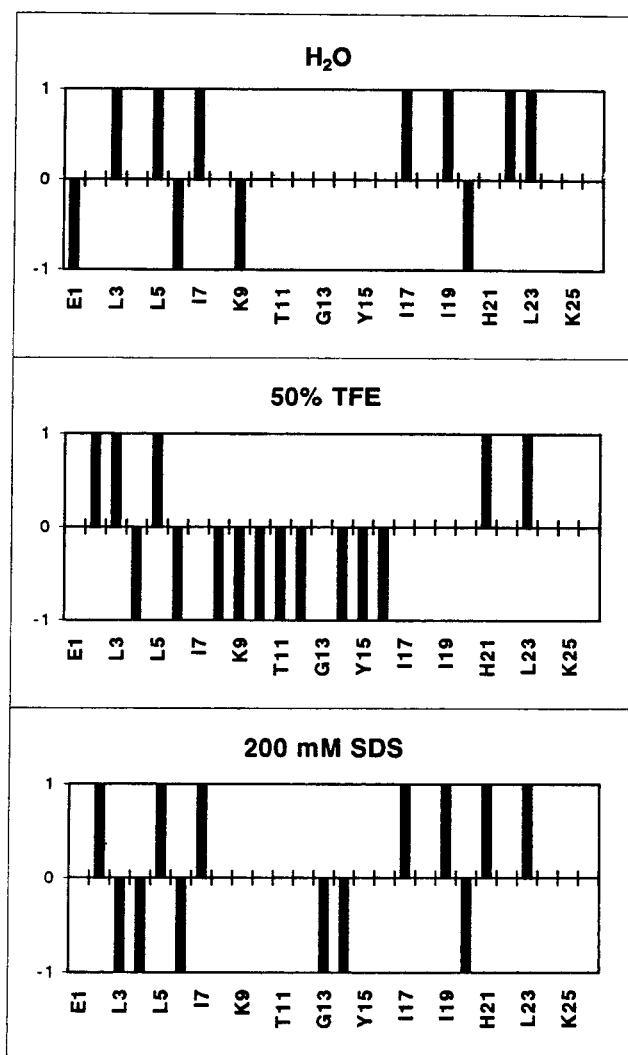


FIGURE 6: Chemical shift index data for LYS(11−36), providing an indication of secondary structure.

β-sheet derived peptide. Again, this is in accord with the CD data.

In 50% TFE, the CSI (Figure 6) indicates the presence of β-turns between residues 4 and 6, followed by a region of helix up until residue 16. A region of random coil was suggested for residues 17−26, although there was some indication of a turn around residue 21. Overall, from the NOE results and chemical shift data, it can be concluded that TFE produces a generally helical structure.

*SDS micelles, 298 K.* The NOEs observed in SDS micelles are summarized in Figure 5C and portions of NOESY spectra are shown in Figure 8. A number of $d_{αN}(i,i + 2)$ and some $d_{αN}(i,i + 3)$ NOEs, as well as medium to strong intensity $d_{αN}(i,i + 1)$ and $d_{NN}(i,i + 1)$ NOEs were observed throughout the peptide. These NOEs are suggestive of interconverting turn-like structures such as nascent or 3₁₀-helices which are in equilibrium with unfolded conformers (Dyson *et al.*, 1988). No ordered helical populations were detected, as evidenced by the lack of $d_{αβ}(i,i + 3)$ connectivities. As with the H₂O, NOE, and chemical shift data, the CSI index for LYS(11−36) in SDS micelles (Figure 6) indicates that some turns may be present near residues 4−7 and 19−21.

## DISCUSSION

We have shown by both CD and NMR spectroscopy, that LYS(11−36) is essentially unstructured in aqueous solution,
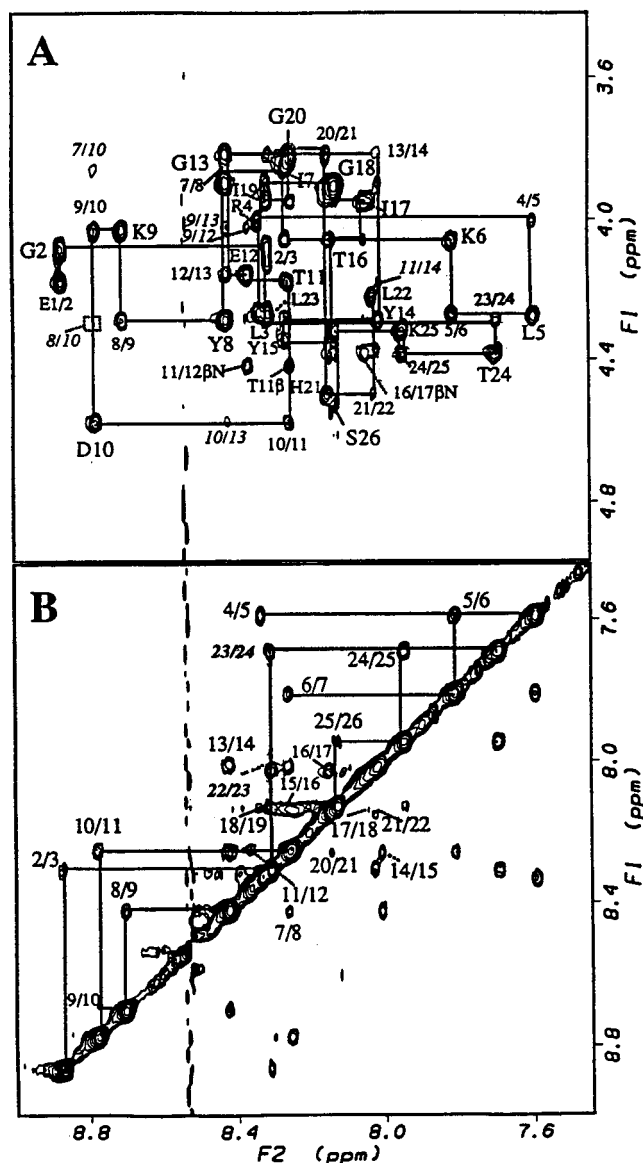
FIGURE 7: Regions of (A) CαH-NH and (B) NH-NH NOESY spectra for LYS(11−36) in 50% TFE/45% 5 mM KPO₄ buffer/5% D₂O (pH 3.35) at 288 K. The sequential assignment and some medium-range NOEs are shown in panel A.

but adopts a helical conformation in 50% TFE and, to a lesser extent, in 200 mM SDS. It is not surprising that the peptide is predominantly unstructured in H₂O as this tendency has been observed for most β-sheet-derived peptides studied in aqueous solution. For example, peptides derived from a β-sandwich protein, plastocyanin (Dyson *et al.*, 1992b), and from the all-β SH3 domain of α-spectrin (Viguera *et al.,* 1996), show little tendency to adopt secondary structure in H₂O. Minor and Kim (1994) have suggested that β-sheet formation is determined, for the most part, by tertiary context, a position supported by Otzen and Fersht, (1995) who stated that β-sheets are formed by the alignment of residues distant in the sequence and that interactions with surrounding residues are likely to play large roles in determining β-sheet propensities. On this basis it is possible that β-sheet formation, in aqueous solution at least, will require relatively large peptide fragments. Certainly, it has proved difficult to use small peptides to study sheet structure as they have tended to self-associate or have solubility problems (Dyson *et al.*, 1992b; Yang *et al.*, 1994).

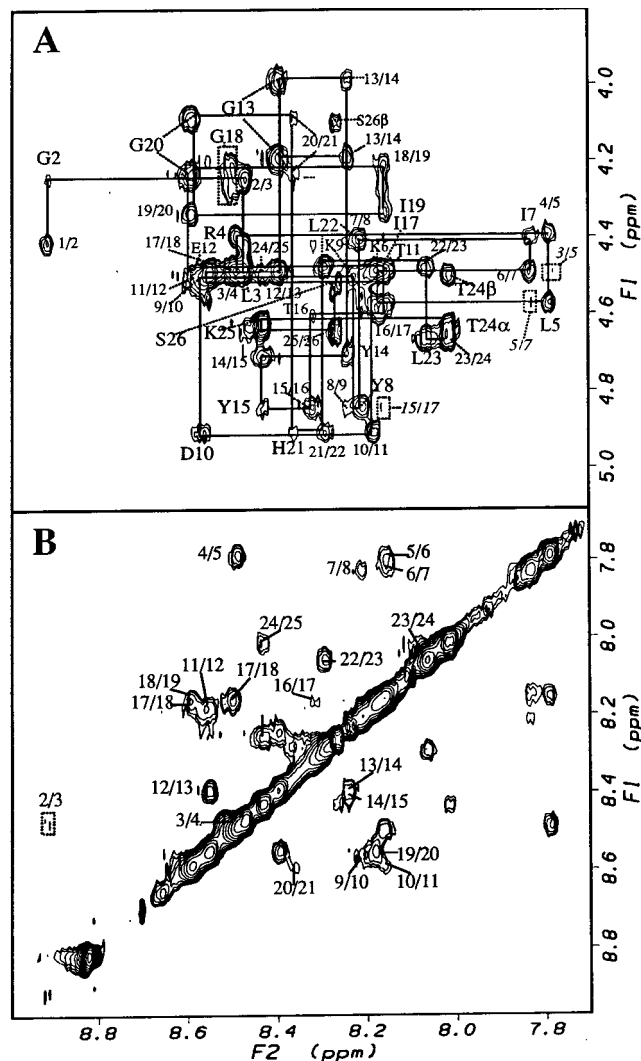The finding that TFE will stabilize a helix in a β-sheet-derived peptide is a more intriguing one, although again not



FIGURE 8: Regions of (A) CαH-NH and (B) NH-NH NOESY spectra for LYS(11−36) in 200 mM SDS micelles (pH 4.5) at 298 K, showing the sequential assignment in panel A.

without precedent. Amyloid β-peptides (Zagorski & Barrow, 1992), a 15-residue β-sheet peptide derived from gp120 (Reed & Kinzel, 1991), peptide fragments of an ice nucleation protein (Ala *et al.*, 1993), a β-strand region from ubiquitin (Muñoz & Serrano,1994), and β-strand fragments derived from β-lactoglobulin, (Hamada *et al.*, 1995) as well as fragments from the SH3 domain of α-spectrin (Viguera *et al.,* 1996), have all demonstrated this ability. Often high (>50%) concentrations of TFE were used, prompting the question as to whether TFE will induce a helical conformation in any given peptide. Although some model studies (Thomas & Dill, 1993) have indicated that all sequences will ultimately become helical in alcohol solutions, there is a substantial body of evidence to indicate that this is not always the case. For example, a number of peptides that correspond to β-sheet, loop, and turn regions of proteins are highly disordered in TFE (Segawa *et al.*, 1991; Sönnichsen *et al.*, 1992; Dyson *et al.* 1992b; Waltho *et al.*, 1993; Shin *et al.*, 1993a,b). In addition, there have been some observations of stable β-sheet (Lu *et al.*, 1984; Martenson *et al.*, 1985; Mutter & Altman, 1985; Narayanan *et al.*, 1986) and β-hairpin (Blanco *et al.*, 1994b; Blanco & Serrano, 1995) structure in TFE. Consequently, it has been suggested that TFE stabilizes α-helical structure only in peptides or protein regions with an inherent helical propensity (Segawa *et al.*,

1991; Sönnichsen *et al.*, 1992; Hamada *et al.*, 1995; Shiraki *et al.*, 1995).

On this basis, the finding that TFE can bring about a helical conformation in LYS(11−36) suggests that the sequence of this peptide possesses an intrinsic helical propensity. Secondary structure predictions (Table 1) show that, in aqueous solution, LYS(11−36) has a propensity for $\beta$-turn/sheet formation from residues 6 to 17. As the hydrophobicity of the solution is increased, the predicted region of turn/sheet is extended to residues 3−18. However, placing the peptide in a fully hydrophobic environment brings about a major change, with helix now being predicted for much of the sequence. This last prediction corresponds to LYS(11−36) being placed in high concentrations of TFE. Interestingly, predictions for LYS(11−36) were in marked contrast with those for LYS(59−81), a peptide derived from a helical region of T4 lysozyme, where a helical conformation was predicted in all environments (McLeish *et al.*, 1994).

Viguera *et al.* (1996) suggest that TFE, in moderate amounts, can reveal low secondary structure propensities of protein fragments, not only for $\alpha$-helical but also for $\beta$-structure. Given the apparent hydrophobicity-based differences in predicted structure for the two T4 lysozyme peptides, it seemed logical to compare their structures under several different hydrophobic conditions. Most helical peptides require about 20−30% TFE to attain maximum helical conformation (Jasanoff & Fersht, 1994) and, as seen from the CD studies summarized in Figure 2, LYS(59−81) clearly falls into that category. By contrast, LYS(11−36) requires at least 40% TFE to form a reasonable helix, and the helical population increases up to 80% TFE. Even then, only about 40% $\alpha$-helical structure is induced, compared to the 55% observed for LYS(59−81) in 50% TFE, as determined from the molar ellipticity at 222 nm. Moreover, the clear isodichroic point in Figure 2B indicates that the folding of LYS(59−81) is a two-state coil-helix process, while the folding of the sheet-derived peptide LYS(11−36) appears to proceed via an intermediate structure. The CD spectrum of this intermediate, apparent at 20% TFE, is not unlike that observed during the TFE titration of an analogous peptide corresponding to the $\beta$-sheet of HEW lysozyme (Yang *et al.*, 1994). In that case, the spectrum was interpreted as indicating that the peptide had "$\beta$-structure" as it was difficult to separate contributions from a variety of $\beta$-sheet and $\beta$-turn structures. CD spectra of $\beta$-sheets show a much greater variability than do those of $\alpha$-helices (Manning *et al.*, 1988), but regardless of exact $\beta$-structure LYS(11−36) adopts, the TFE titration results appear to substantiate the differences in secondary structure predicted for the two peptides. This not only supports the hypothesis of Jasanoff and Fersht (1994) that TFE titrations can be used as probes for a peptide's helical tendencies but also that of Viguera *et al.* (1996) that moderate amounts of TFE can reveal a propensity for $\beta$-structure.

In addition to TFE, SDS micelles have also been used to provide a hydrophobic environment and to mimic biological membranes. Since the structural propensities of LYS(11−36) and LYS(59−81) seemed to be identifiable by TFE titration, we decided to determine whether the peptides would adopt different conformations in micellar, and nonmicellar, SDS. Micellar SDS has been used to stabilize $\alpha$-helices in a range of peptides including gastrin analogues (Mammi & Peggion, 1990), bombolitins (Bairaktari *et al.*, 1990), uteroglobin fragments (Tessari *et al.*, 1993), and, in our previous

studies, T4 lysozyme fragments (McLeish *et al.*, 1993, 1994). While these fragments were derived from helical regions of proteins, it has been shown that peptides derived from regions of $\beta$-sheet (Zhong & Johnson, 1992) as well as peptides predicted to be $\beta$-strand (Waterhous & Johnson, 1994) could also form stable helices in micellar SDS. In addition, the latter studies indicated that the sheet peptides were able also to form $\beta$-strands when placed in nonmicellar SDS (Zhong & Johnson, 1992; Waterhous & Johnson, 1994).

Figure 3 shows that at higher SDS concentrations both peptides form $\alpha$-helices. Below the critical micellar concentration, LYS(11−36) formed stable $\beta$-structures, while LYS(59−81) maintained its helical conformation until it aggregated at around 1 mM SDS. This is in accord with Wu *et al.* (1981), who proposed that at low molar surfactant/ peptide ratio, $\beta$-structure may exist if the peptide has $\beta$-forming potential. Excess surfactant usually was able to disrupt the $\beta$-form and, if the peptide had helix forming potential, could convert it into a helix. To date, the specific interactions between peptides and SDS micelles which induce $\alpha$-helical structure have not been identified, although Wu *et al.* (1982) suggested that, after an initial electrostatic interaction, the micellar amphiphiles cluster around the peptide, thereby providing a hydrophobic environment that supports an ordered conformation that otherwise would have been disrupted by peptide backbone−water interactions. For $\beta$-structures, Zhong and Johnson (1992) proposed that the hydrophobic tail mimics the environment found in the protein interior while the hydrophilic end of the SDS molecule is able to keep the $\beta$-structure in solution.

The NMR studies, in general, confirm the CD results for LYS(11−36) in water, in 50% TFE, and in SDS micelles. Both the NOE and chemical shift data are consistent with the peptide adopting a predominantly extended conformation in aqueous solution, with some turns present near residues 4−5 and 18−21. In accord with the CD data, following the addition of 50% TFE, LYS(11−36) shows a strong helical propensity as indicated by observation of strong $d_{NN}(i,i + 1)$ NOEs, appearance of many medium-range NOEs and a number of slowly exchanging NH protons. Chemical shifts also support helical conformations in TFE. For LYS(11− 36) in SDS micelles, the NOE data was more indicative of turn-like or nascent helical structures as seen by the appearance of many $d_{\alpha N}(i,i + 2)$ and $d_{\alpha N}(i,i + 3)$ NOEs. The lack of observation of strong $d_{NN}(i,i + 1)$ and $d_{\alpha\beta}(i,i + 3)$ NOEs indicates that the helical populations are not fully ordered. The turn, centered on residue 19, that was observed in $H_2O$ was also supported by the CSI in SDS micelles. Interestingly, this turn is present in the corresponding region of crystal structure of T4 lysozyme.

Attempts to obtain NMR structural data on LYS(11−36) in nonmicellar SDS were unsuccessful. Broad spectra were obtained, presumably due to aggregation at the higher concentrations of peptides, relative to the CD studies, necessary to obtain NMR data.

*Implications for T4 Lysozyme Folding.* Both HD exchange studies (Lu & Dahlquist, 1992) and structure-based predictions (Xie & Freire, 1994) have implicated the $\beta$-sheet in the early events in T4 lysozyme folding. As shown in Figure 9, in the native protein there are two turns connected by three strands to form a triple-stranded antiparallel $\beta$-sheet (Remington *et al.*, 1978; Weaver & Matthews, 1987). The two turns, involving residues Asp20-Thr21-Glu22-Gly23 and Gly28-Ile29-Gly30 have been described as type 1 and
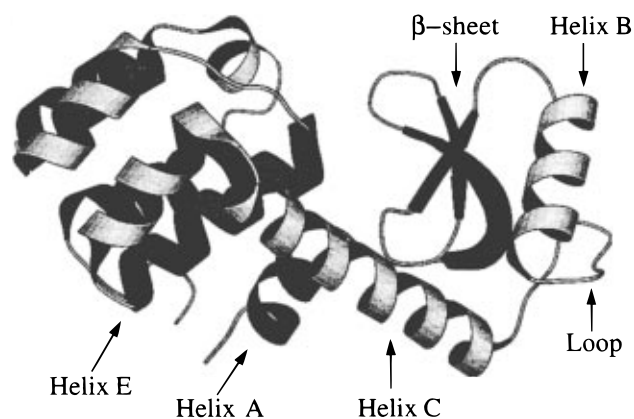
FIGURE 9: Ribbon diagram of the crystal structure of T4 lysozyme generated by Molscript (Kraulis, 1991) showing the $\beta$-sheet region and its proximity to the loop and helices A, B, C, and E.

irregular, respectively (Remington *et al.*, 1978). The X-ray structure shows that the $\beta$-sheet makes as many as 30 close (within 5 Å) contacts with other secondary segments (Remington *et al.*, 1978; Weaver & Matthews, 1987). While most of these contacts are with helix B and the loop which, together with the sheet region, form part of an $(\alpha + \beta)$ domain, there are also a number of contacts with helices A and E. In addition, there is a strong salt-bridge between the $\beta$-sheet residue His31 and Asp70 located in helix C which contributes 3−5 kcal/mol toward the stabilization of the native structure (Anderson *et al.*, 1990). While clearly these contacts are important in maintaining the stability of the $\beta$-sheet, it is not so clear as to whether some or all of the contacts are necessary to drive the formation of the $\beta$-sheet. Nonetheless, it is interesting to note that these three helices have all been shown to form rapidly, and have been proposed as initiation sites for T4 lysozyme folding (Lu & Dahlquist, 1992; Xie & Friere, 1994).

A recent study by Blanco *et al.* (1994a) showed that, in aqueous solution, a 16 residue peptide fragment from the B1 domain of protein G adopted a native-like $\beta$-hairpin structure. This hairpin was further stabilized in 30% TFE/70% $H_2O$ (Blanco & Serrano, 1995), and it was suggested that it may provide a folding initiation site for protein G. Similarly, aqueous TFE solutions have been reported to stabilize turns in isolated actin (Sönnichsen *et al.*, 1992) and myoglobin (Shin *et al.*, 1993a) fragments with, in the latter case, the possibility of the turn being an initiation site also being raised. In the present study, there is strong evidence for LYS(11−36) residues G18-I19-G20-H21 forming a turn in water, in SDS micelles and, to a lesser extent, in 50% TFE. In T4 lysozyme these residues correspond to the region Gly28-Ile29-Gly30-His31, which includes the irregular turn (Remington *et al.*, 1978). When combined with the HD exchange studies, which found that Gly28 and Ile29 had protection factors well in excess of 20 (Lu & Dahlquist, 1992), our results certainly suggest that formation of this turn is one of the earliest events in lysozyme folding.

The results of the titration experiments indicate that the amino acid sequence plays the major part in determining which secondary structure is formed for LYS(59−81), while for LYS(11−36) the peptide environment plays the dominant role. In these experiments we have seen LYS(11−36) adopt an extended conformation, a $\beta$-sheet conformation, or an $\alpha$-helical conformation, depending on the solution conditions. Of particular interest is the ability of LYS(11−36) to undergo a reversible solvent-induced $\beta$-sheet to $\alpha$-helix transition.

Such a transition has been reported for a number of peptides, including the analogous sheet peptide from HEW lysozyme (Yang, *et al.*, 1994) as well as for intact proteins. Liu *et al.* (1994) suggest that the unfolded polypeptide chain has a much greater tendency for formation of helix rather than $\beta$-sheet, and it is possible that, for T4 lysozyme, a transient non-native $\alpha$-helix is initially formed which, after some stabilizing, longer-range tertiary contacts are established, then rapidly converts to a $\beta$-sheet. Such non-native $\alpha$-helical intermediate formation, prior to $\beta$-sheet formation, has been suggested for two predominantly $\beta$-sheet proteins: the cellular retinoic acid binding protein (Liu *et al.*, 1994) and $\beta$-lactoglobulin (Shiraki *et al.*, 1995; Hamada *et al.*, 1995). Recently, Shiraki *et al.* (1995) and Hamada *et al.* (1995) proposed that $\beta$-sheet formation via $\alpha$-helical intermediates suggests a nonhierarchical protein folding (Lim, 1978; Goldenberg, 1992), wherein localized hydrogen bonding may give rise to accumulation of a nonnative $\alpha$-helical intermediate early in the folding. As longer range interactions begin to predominate, the helix is disrupted or rearranged in order for the protein to fold into the native $\beta$-sheet structure. To date there is still limited information about $\beta$-sheet formation via $\alpha$-helical intermediates, and such speculations are a subject of much debate (Weissman & Kim, 1991; Matthews, 1993; Varley *et al.*, 1993).

However, there is one piece of evidence which would mitigate against this being the case for T4 lysozyme. The HD exchange experiments of Lu and Dahlquist (1992) indicate that the $\beta$-sheet region forms rapidly, within 8 ms of folding, as a somewhat isolated region of secondary structure. It is unlikely that an $\alpha$-helix could form and convert to a $\beta$-sheet within this time frame and without undergoing HD exchange. By contrast, the $\beta$-sheet domain of HEW lysozyme is unable to protect amides from exchange in the absence of stable, structured $\alpha$-domain, and the formation of the $\beta$-domain is one of the slowest events on the folding pathway (Yang *et al.*, 1994). This is possibly due to a transient population of nonnative structure in the $\beta$-sheet region (Buck *et al.*, 1995) a suggestion more consistent with the $\beta$-sheet formation via $\alpha$-helical intermediates scenario described earlier.

In conclusion, we have demonstrated that LYS(11−36), a peptide derived from the $\beta$-sheet region of T4 lysozyme is able to adopt a nonnative helical conformation in 50% TFE and, to a lesser extent, in SDS micelles. TFE and SDS titrations have been used to test and confirm structure predictions which indicate that the peptide has a propensity for $\beta$-structure in hydrophilic solution and $\alpha$-helical propensity in hydrophobic solution. There is evidence that small populations of a 'native-like' turn were present, even in aqueous solution. The fact that this turn persists in the absence of stabilizing tertiary interactions suggests that it may form a nucleation site for the folding of the sheet region of T4 lysozyme. This lends credence to earlier theoretical and experimental studies which indicate that the sheet region forms part of an early folding intermediate.

## SUPPORTING INFORMATION AVAILABLE

A table of chemical shift assignments for LYS(11−36) in the three solvents (6 pages). Ordering information is given on any current masthead page.

## REFERENCES

Ala, P., Chong, P., Ananthanarayanan, V. S., Chan, N., & Yang, D. S. C. (1993) *Biochem. Cell Biol. 71*, 236−246.

Anderson, D. E., Becktel, W. J., & Dahlquist, F. W. (1990) *Biochemistry 29*, 2403−2408.

Anfinsen, C. B. (1973) *Science 181*, 223−230.

Bairaktari, E., Mierke, D. F., Mammi, S., & Peggion, E. (1990) *Biochemistry 29*, 10090−10096.

Bandekar, J., Evans, D. J., Krimm, S., Leach, S. J., Lee, S., McQuie, J. R., Minasian, E., Nemethy, G., Pottle, M. S., Scheraga, H. A., Stimson, E. R., & Woody, R. W. (1982) *Int. J. Peptide Protein Res. 19*, 187−205.

Bax, A., & Davis, D. G. (1985) *J. Magn. Reson. 65*, 355−360.

Blanco, J. F., & Serrano, L. (1995) *Eur. J. Biochem. 230*, 634−649.

Blanco, J. F., Rivas, G., & Serrano, L. (1994a) *Nat. Struct. Biol. 1*, 584−590.

Blanco, J. F., Jiménez, A., Pineda, A., Rico, M., Santoro, J., & Nieto, J. L. (1994b) *Biochemistry 33*, 6004−6014.

Braünschweiler, L., & Ernst, R. R. (1983) *J. Magn. Reson. 53*, 521−528.

Buck, M., Schwalbe, H., & Dobson, C. M. (1995) *Biochemistry 34*, 13219−13232.

Cavanagh, J., & Rance, M. (1992) *J. Magn. Reson. 96*, 670−678.

Chen, Y.-H., Yang, J. T., & Chau, K. H. (1974) *Biochemistry 13*, 3350−3359.

Dyson, H. J., & Wright, P. E. (1991) *Annu. Rev. Biophys. Chem. 20*, 519−538.

Dyson, H. J., & Wright, P. E. (1993) *Curr. Opin. Struct. Biol. 3*, 60−65.

Dyson, H. J., Cross, K. J., Houghten, R. A., Wilson, I. A., Wright, P. E., & Lerner, R. A. (1985) *Nature 318*, 480−483.

Dyson, H. J., Rance, M., Houghten, R. A., Wright, P. E., & Lerner, R. A. (1988) *J. Mol. Biol. 201*, 201−217.

Dyson, H. J., Merutka, G., Waltho, J. P., Lerner, R. A., & Wright, P. E. (1992a) *J. Mol. Biol. 226*, 795−817.

Dyson, H. J., Sayre, J. R., Merutka, G., Shin, H.-C., Lerner, R. A., & Wright, P. E. (1992b) *J. Mol. Biol. 226*, 819−835.

Gierasch, L. M. *Biochemistry 28*, 923−930.

Goldenberg, D. P. (1992) *Trends Biochem. Sci. 17*, 257−261.

Hamada, D., Kuroda, Y., Tanaka, T., & Goto, Y. (1995) *J. Mol. Biol. 254*, 737−746.

Jasanoff, A., & Fersht, A. R. (1994) *Biochemistry 33*, 2129−2135.

Kemmink, J., & Creighton, T. E. (1995) *Biochemistry 34*, 12630−12635.

Kim, P. S., & Baldwin, R. L. (1982) *Annu. Rev. Biochem. 51*, 459−489.

Kim, P. S., & Baldwin, R. L. (1990) *Annu. Rev. Biochem. 59*, 631−660.

Kim, P. S., Bierzynski, A., & Baldwin, R. L. (1982) *J. Mol. Biol. 162*, 187−199.

Kraulis, P. J. (1991) *J. Appl. Crystallogr. 24*, 946−950.

Kumar, A., Ernst, R. R., & Wüthrich, K. (1980) *Biochem. Biophys. Res. Commun. 95*, 1−6.

Lim, V. I. (1978) *FEBS Lett. 89*, 10−14.

Liu, Z.-P., Rizo, J., & Gierasch, L. M. (1994) *Biochemistry 33*, 134−142.

Lu, J., & Dahlquist, F. W. (1992) *Biochemistry 31*, 4749−4756.

Lu, Z. X., Fok, K. F., Ericson, B. W., & Hugli, T. E. (1984) *J. Biol. Chem. 259*, 7367−7370.

Mammi, S., & Peggion, E. (1990) *Biochemistry 29*, 5265−5269.

Manning, M. C., Illangasare, M., & Woody, R. W. (1988) *Biophys. Chem. 31*, 77−86.

Martenson, R. E., Park, J. Y., & Stone, A. L. (1985) *Biochemistry 24*, 7689−7695.

Matthews, B. W. (1993) *Annu. Rev. Biochem. 62*, 139−160.

McLeish, M. J., Nielsen, K. J., Wade, J. D., & Craik, D. J. (1993) *FEBS Lett. 315*, 323−328.

McLeish, M. J., Nielsen, K. J., Najbar, L. V., Wade, J. D., Lin, F., Doughty, M. B., & Craik, D. J. (1994) *Biochemistry 33*, 11174−11183.

Minor, D. L., & Kim, P. S. (1994) *Nature 371*, 264−267.

Muñoz, V., & Serrano, L. (1994) *Nat. Struct. Biol. 1*, 399−409.

Mutter, M., & Altman, K.-H. (1985) *Int. J. Pept. 26*, 373−380.

Najbar, L. V., Craik, D. J., Wade, J. D., Lin, F., & McLeish, M. J. (1995) *Biochim. Biophys. Acta 1250*, 163−170.

Narayanan, U., Keiderling, T. A., Bonora, G. M., & Toniolo, C. (1986) *J. Am. Chem. Soc. 108*, 2431−2437.

Oas, T. G., & Kim, P. S. (1988) *Nature 336*, 42−48.

Otzen, D. E., & Fersht, A. R. (1995) *Biochemistry 34*, 5718−5724.

Plateau, P., & Gueron, M. (1982) *J. Am. Chem Soc. 104*, 7310−7311.

Ptitsyn, O. B., & Finkelstein, A. V. (1983) *Biopolymers 22*, 15−25.

Rance, M., Sørensen, O. W., Bodenhausen, G., Wagner, G., Ernst, R. R., & Wüthrich, K. (1983) *Biochem. Biophys. Res. Commun. 117*, 479−485.

Rao, S., Zhu, Q.-L., Vajda, S., & Smith, T. (1993) *FEBS Lett. 322*, 143−146.

Reed, J., & Kinzel, V. (1991) *Biochemistry 30*, 4521−4528.

Remington, S. J., Anderson, W. F., Owen, J., Ten Eyck, L. F., Grainger, C. T., & Matthews, B. W. (1978) *J. Mol. Biol. 118*, 81−98.

Rizo, J., Blanco, F. J., Kobe, B., Bruch, M. D., & Gierasch, L. M. (1993) *Biochemistry 32*, 4881−4894.

Segawa S. I., Fukuno, T., Fujiwara, K., & Noda, Y. (1991) *Biopolymers 31*, 497−509.

Shin, H.-C., Merutka, G., Waltho, J. P., Wright, P. E., & Dyson, J. H. (1993a) *Biochemistry 32*, 6348−6355.

Shin, H.-C., Merutka, G., Waltho, J. P., Tennant, L. L., Dyson, J. H., & Wright, P. E. (1993b) *Biochemistry 32*, 6356−6364.

Shiraki, K., Nishikawa, K., & Goto, Y. (1995) *J. Mol. Biol. 245*, 180−194.

Sönnichsen, F. D., Van Eyk, J. E., Hodges, R. S., & Sykes, B. D. (1992) *Biochemistry 31*, 8790−8798.

Tessari, M., Foffani, M. T., Mammi, S., & Peggion, E. (1993) *Biopolymers 33*, 1877−1887.

Thomas, P. D., & Dill, K. A. (1993) *Protein Sci. 2*, 2050−2065.

Varley, P., Gronenborn, A. M., Christensen, H., Wingfield, P., Pain, R. H., & Clore, G. M. (1993) *Science 260*, 1110−1113.

Viguera, A. R., Jiménez, M. A., Rico, M., & Serrano, L. (1996) *J. Mol. Biol. 255*, 507−521.

Wade, J. D., Perich, J. W., McLeish, M. J., Otvos, L., Jr., & Tregear, G. W. (1995) *Lett. Pept. Sci. 2*, 71−76.

Waltho, J. P., Feher, V. A., Merutka, G., Dyson, H. J., & Wright, P. E. (1993) *Biochemistry 32*, 6337−6347.

Waterhous, D. V., & Johnson, W. C. (1994) *Biochemistry 33*, 2121−2128.

Weaver, L. H., & Matthews, B. W. (1987) *J. Mol. Biol. 193*, 189−199.

Weissman, J. S., & Kim, P. S. (1991) *Science 253*, 1386−1393.

Wishart, D. S., Sykes, B. D., & Richards, F. M. (1991) *J. Mol. Biol. 201*, 201−217.

Wishart, D. S., Sykes, B. D., & Richards, F. M. (1992) *Biochemistry 31*, 1647−1651.

Woody, R. W. (1985) in *The Peptides* (Hruby, V., Ed.) Academic Press, New York.

Wright, P. E., Dyson, H. J., & Lerner, R. A. (1988) *Biochemistry 20*, 7167−7175.

Wu, C.-S., Ikeda, K., & Yang, J. T. (1981) *Biochemistry 20*, 566−570.

Wu, C.-S., Hachimori, A., & Yang, J. T. (1982) *Biochemistry 21*, 4556−4562.

Wüthrich, K. (1986) *NMR of Proteins and Nucleic Acids* John Wiley & Sons Inc., New York.

Xie, D., & Freire, E. (1994) *J. Mol. Biol. 242*, 62−80.

Yang, J. J., Pitkeathly, M., & Radford, S. E. (1994) *Biochemistry 33*, 7345−7353.

Zagorski, M. G., & Barrow, J. (1992) *Biochemistry 31*, 5621−5631.

Zhong, L., & Johnson, W. C., Jr. (1992) *Proc. Natl. Acad. Sci. U.S.A. 89*, 4462−4465.